

Critical Role of Diffraction Simulation in Establishing the Crystal and Molecular Structures of Poly(biaryl ether ketone)s

Peter L. Aldred and Howard M. Colquhoun*

Department of Chemistry, University of Reading, Whiteknights, Reading RG6 6AD, UK

David J. Williams*

Department of Chemistry, Imperial College, South Kensington, London SW7 2AY, UK

David J. Blundell*

Department of Physics, Keele University, Keele, Staffs ST5 5BG, UK

Received June 11, 2002

ABSTRACT: Molecular modeling and diffraction simulation studies of the biphenyl-based poly(ether ketone)s $[\text{O}-\text{Ar}-\text{Ar}-\text{O}-\text{Ar}-\text{CO}-\text{Ar}-\text{Ar}-\text{CO}-\text{Ar}]_n$ (**3**) and $[-\text{O}-\text{Ar}-\text{Ar}-\text{CO}-\text{Ar}-]_n$ (**4**, Ar = 1,4-phenylene), coupled with data obtained from an oligomer single-crystal study, have enabled their crystal and molecular structures to be determined from X-ray powder data. A crystallographically disordered structure in which the ether and ketone linkages are distributed randomly over the bridging positions of the polymer chain is potentially available to both polymers and undoubtedly occurs in their random 1:2 copolymer (**5**). The disordered structure is monoclinic (rather than orthorhombic as has previously been proposed), in space group $P2_1/b$, with two chains per unit cell. Rietveld refinement of this structure for polymers **3** and **4**, based on X-ray powder data, gave final agreement factors (R_{wp}) of 5.7% and 6.6%, respectively. Analysis of X-ray fiber data by diffraction simulation methods suggests that the disordered structure always predominates for **3** but that a partially ordered arrangement of ether and ketone linkages is present in oriented samples of polymer **4**.

Introduction

Structural analysis of main-chain aromatic polymers is rarely straightforward, as their crystallite dimensions are generally no larger than a few tens of nanometers and so give rise to broad and often overlapping X-ray diffraction peaks. Even when two-dimensional diffraction data are obtained from oriented films or fibers, the number of unique reflections observed is generally much smaller than the number of independent structural parameters. Bond lengths and angles thus have to be tightly constrained in any crystallographic analysis, and the conformation of the polymer chain and its mode of crystal packing must be restricted to only a very small range of possible options.

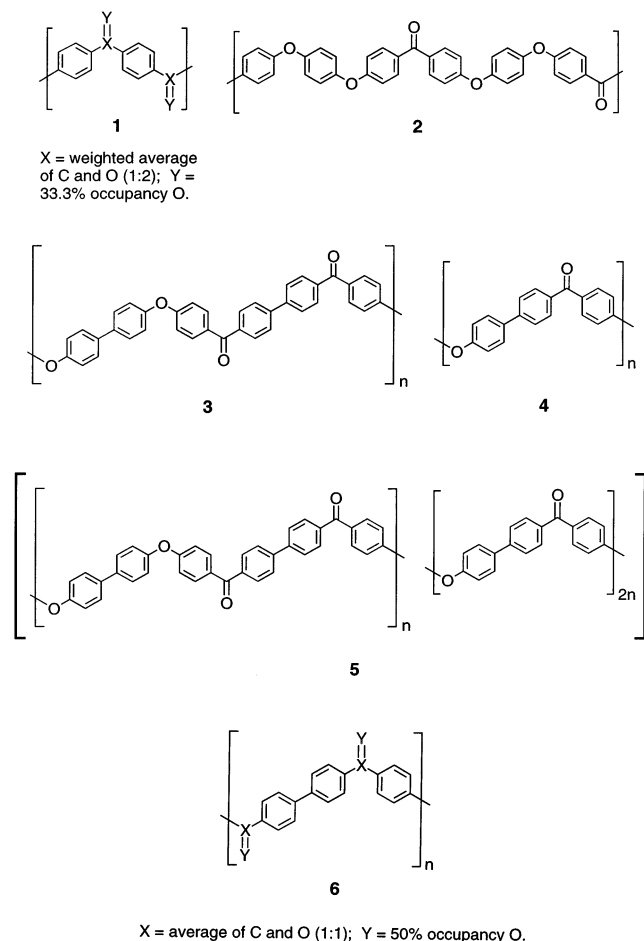
We have recently shown that these limitations can, to a large extent, be overcome by a modification of the interactive diffraction modeling technique originally developed by Windle and co-workers.¹ This modified approach² depends on the availability of single-crystal X-ray data for an oligomer analogue of the polymer in question. Such data may then be used not only to construct realistic trial models for the polymer crystal but also to reparametrize a molecular mechanics force field so as to accurately reproduce the crystal structure of the oligomer. In this way a high degree of confidence can be placed on the initial choice of polymer model and also on the ability of molecular mechanics energy minimization to deliver realistic results. Diffraction simulation is used to identify promising trial structures, so enabling the calculation of potential unit cell parameters (which for polymer structures are rarely accessible by direct indexing of the powder pattern). Energy minimization of the polymer chain conformation and crystal packing can thus be subsequently carried out within an experimentally determined unit cell, and analysis of the symmetry elements present in the

structure allows the space group to be assigned. Finally, the model structure can often be refined with reference to the experimental powder pattern using Rietveld methods, though this is not always possible if peak overlap is very extensive.

For aromatic polymers, it is generally accepted that ether and ketone linkages are essentially equivalent in geometric terms;³ bond angles at both are ca. 121°, C–O and C–C bond distances are similar at 1.386 and 1.486 Å, respectively, and the torsion angle relating the plane of either bridging unit to its adjoining aromatic ring is normally in the range 30°–34°. Single-crystal studies of aromatic ether ketone oligomers have shown that chain packing is dominated by aromatic edge-to-face contacts and that interchain $\text{O}_{\text{ether}} \cdots \text{O}_{\text{ether}}$ and $\text{C}_{\text{carbonyl}} \cdots \text{C}_{\text{carbonyl}}$ separations are essentially identical.⁴ As a result, there exists a vacant site adjacent to every ether oxygen atom which could equally well be occupied by a ketonic oxygen, *without* perturbation of the crystal lattice. The ether and ketone linking units can thus be regarded as crystallographically interchangeable, and disordered structures are to be expected for aromatic poly(ether ketone)s such as PEEK. This polymer does in fact crystallize in space group $Pbcn$ with a disordered two-ring crystallographic repeat (**1**) rather than the six-ring repeat (**2**) which would be required in a fully ordered crystal.³

We have already proposed from DSC studies that aromatic poly(ether ketone)s containing *biphenyl* linkages can adopt similarly disordered structures (**6**), since *random copolymers* of the repeat units $[-\text{O}-\text{Ar}-\text{Ar}-\text{O}-\text{Ar}-\text{CO}-\text{Ar}-\text{Ar}-\text{CO}-\text{Ar}]_n$ (**3**, Ar = 1,4-phenylene) and $[-\text{O}-\text{Ar}-\text{Ar}-\text{CO}-\text{Ar}-]_n$ (**4**) do not differ significantly from their parent homopolymers, either in melting point or enthalpy of fusion.⁵ The same proposal of crystallographic ether/ketone disorder has also more

recently been made for this family of polymers based on the similarity of their X-ray powder patterns, which were indexed in terms of a hypothetical orthorhombic unit cell.⁶ In the present paper, we analyze X-ray powder and fiber data for polymers **3**, **4**, and their 1:2 random copolymer (**5**) using diffraction simulation methods and show that although a disordered model (in fact, based on a monoclinic rather than an orthorhombic unit cell) satisfactorily accounts for the diffraction data for **3** and **5**, an at least partially ordered structure is present in oriented samples of polymer **4**.



Experimental Section

Synthesis of Polymers 3–5 (Nucleophilic Method). Polymer **3** was obtained by condensation of 4,4'-bis(4-fluorobenzoyl)biphenyl^{4a} (1.462 g, 3.67 mmol) with 4,4'-biphenyldiol (0.615 g, 3.30 mmol) in diphenyl sulfone (7.40 g) as solvent, in the presence of anhydrous sodium carbonate (0.360 g, 3.40 mmol). The reaction mixture was stirred under nitrogen and heated to 325 °C over about 2 h and then held at this temperature for a further 3 h under conditions of slow nitrogen purge. The suspension of polymer and salts was then cooled to 200 °C and poured onto a sheet of aluminum foil. After solidification the product was milled to a coarse powder and extracted three times with acetone at reflux and then three times with boiling water, before finally drying under vacuum at 80 °C overnight. The yield of polymer **3** was 1.34 g (75%). The melting point (DSC, 10 °C min⁻¹) was 464 °C, and the inherent viscosity (η_{inh}) at 0.1% concentration in 98% sulfuric acid was 0.18 dL g⁻¹. Polymer **4** (mp 466 °C, η_{inh} 0.14 dL g⁻¹) was prepared under essentially identical conditions by self-condensation of 4-(4-fluorobenzoyl)-4'-hydroxybiphenyl,⁷ and polymer **5** was obtained by co-condensation of the latter monomer with 4,4'-bis(4-fluorobenzoyl)biphenyl and 4,4'-biphenyldiol, in a molar ratio of 2:1:1, respectively.

Synthesis of Polymers 3–5 (Electrophilic Method). High molar mass samples of these polymers were obtained by electrophilic polycondensations in trifluoromethanesulfonic acid, as described in an earlier paper.⁵ Fibers were wet-spun directly from these reactions into water and were then washed exhaustively with boiling water and then ethanol, treated with DMAc at reflux, oriented by drawing to ca. 3.5 times their original length at 400 °C in air, and then annealed at constant length at 325 °C for 18 h under nitrogen.

Synthesis of Oligomer 10. Benzoic acid (0.366 g, 3.00 mmol) and 4,4'-diphenoxybiphenyl (0.306 g, 1.00 mmol) were dissolved in trifluoromethanesulfonic acid (5.0 mL) under dry nitrogen and were allowed to react for 18 h. The deep orange solution was poured into water, and after stirring for 30 min, the precipitated white solid was filtered off, washed with boiling water and then with ethanol, and recrystallized from dimethylformamide. Yield was 0.477 g, (88%); mp 265 °C (lit. 268 °C).⁸

Crystallographic Methods. Single crystals of oligomer **10** were grown by very slow cooling of a dilute solution in dimethylformamide, and X-ray data for this compound were measured on a Nicolet R3m/E diffractometer with graphite-monochromated Cu K α radiation (λ = 1.5418 Å) using ω -scans. The structure was solved using the SHELXTL-PC program system.

Crystal Data for Oligomer 10. C₃₈H₂₆O₄: monoclinic, space group $P2_1/n$, a = 6.042(1), b = 7.561(1), c = 59.246(8) Å, β = 92.14(1)°, V = 2704.7(6) Å³, Z = 4, D_c = 1.342 g cm⁻³, μ (Cu K α) = 6.88 cm⁻¹, T = 293 K. Independent reflections measured 3397, R_1 = 0.0482, wR_2 = 0.1240 for 1966 independent observed reflections [$F > 4\sigma(F)$]. Full crystallographic details for this structure are available as Supporting Information.

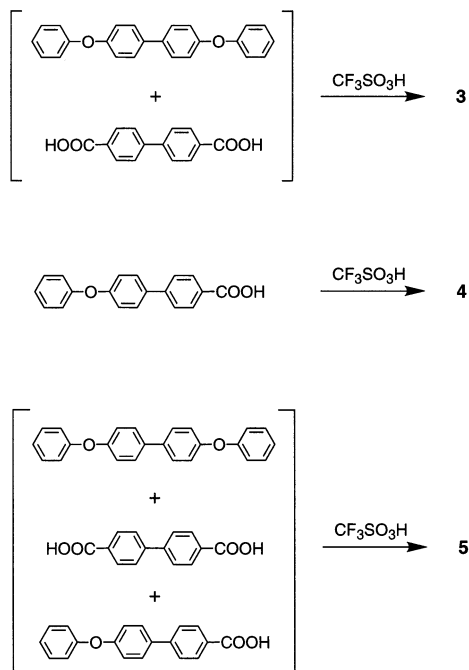
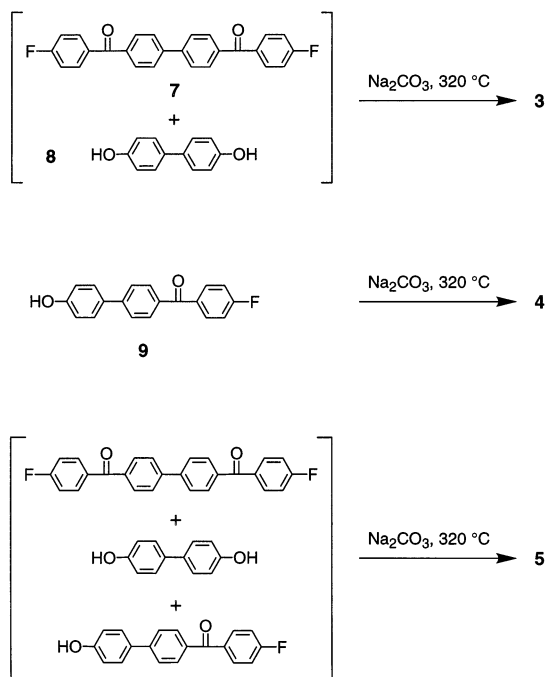
X-ray powder data were obtained using Cu K α radiation on a Bruker D5000 instrument (Bragg–Brentano geometry) and also at the CCLRC-Daresbury Synchrotron Radiation Source (capillary geometry). Flat-plate fiber data were obtained using the same synchrotron source, at a wavelength of 1.488 Å. Computational model building, diffraction simulation, and crystallographic refinement from powder data were carried out using the program systems Cerius2 (v. 3.5) and Materials Studio (v. 1.2), both from Accelrys Inc., San Diego.

Structure Determination for Polymers 3 and 4 (Disordered Model). Polymer **3**: [C₁₉H₁₂O₂]_{2n}, M = (272.30)_{2n}, monoclinic, space group $P2_1/b$, a = 7.560(1), b = 6.085(1), c = 14.040(1) Å, α = 96.70(1)°, V = 641.5 (3) Å³, Z = 2, T = 298 K, D_c = 1.39 g cm⁻³. Powder data collection range, 2θ = 5.50°–49.50°, step size 0.028°, Cu K α , λ = 1.542 Å. Peak profile function: Thompson–Cox–Hastings, U = 0.1940, V = 0.4551, W = -0.0255, X = 0.2688, Y = -0.2753, Z = -0.0003. Peak asymmetry correction: Berar–Baldinozzi, $P1$ = -0.9236, $P2$ = -0.1526, $P3$ = 1.7776, $P4$ = 0.2897 (all parameters as defined in Materials Studio v. 1.2) Polymer crystallite dimensions: a = 130, b = 150, c = 80 Å. Lattice strain: a = 0.115, b = 0.014, c = 0%. Zero point correction, 0.0092°. Agreement factors: R_{wp} = 0.057, R_p = 0.123.

The same disordered model was refined against the X-ray powder profile for polymer **4**: [C₁₉H₁₂O₂]_n, M = (272.30)_n, monoclinic, space group $P2_1/b$, a = 7.565(1), b = 6.008(1), c = 14.087(1) Å, α = 96.80(1)°, V = 6635.8 (3) Å³, Z = 2, T = 298 K, D_c = 1.42 g cm⁻³. Powder data collection range, 2θ = 5.00°–50.00°, step size 0.020°, synchrotron radiation, λ = 1.400 Å. Peak profile function: Thompson–Cox–Hastings, U = 0.1447, V = 0.3800, W = 0.0500, X = 0.0606, Y = -0.1775, Z = -0.0692. Peak asymmetry correction: Berar–Baldinozzi, $P1$ = 0.0278, $P2$ = 0.0817, $P3$ = 0.0186, $P4$ = -0.1828. Polymer crystallite dimensions: a = 110, b = 190, c = 80 Å. Lattice strain: a = 0.115, b = 0.014, c = 0%. Zero point correction, -0.0711°. Agreement factors: R_{wp} = 0.066, R_p = 0.117.

Results and Discussion

Polymers **3–5** were synthesized by both the originally reported electrophilic method (Scheme 1)⁵ and also by

Scheme 1. Electrophilic Syntheses Affording Poly(ether ketone)s 3–5 at High Molar Mass**Scheme 2. Nucleophilic Polycondensations Giving Low Molar Mass Polymers**

nucleophilic polycondensation (Scheme 2). For polymer **3**, the nucleophilic approach involved reaction of 4,4'-bis(4-fluorobenzoyl)biphenyl (**7**) with 4,4'-biphenyldiol (**8**) at 325 °C in diphenyl sulfone as solvent. Polymer **4** was similarly obtained by self-polycondensation of 4-(4-fluorobenzoyl)-4'-hydroxybiphenyl (**9**). Nucleophilic polymerizations gave materials of high crystallinity, affording well-resolved wide-angle X-ray powder patterns (Figure 1), but these polymers were of relatively low molar mass (inherent viscosities, η_{inh} , 0.12–0.18 dL g⁻¹), reflecting their extreme insolubility in the reaction solvent, even at very high temperatures (up to 325 °C). In the synthesis of polymer **3**, use of either a 2% or 10% molar excess of the difluoro-monomer **7** gave polymer

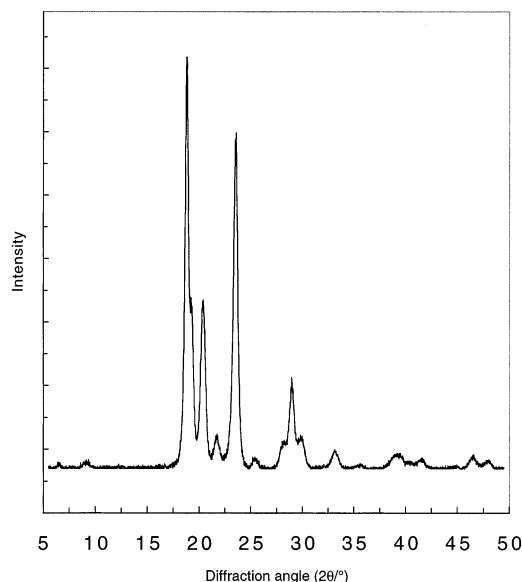
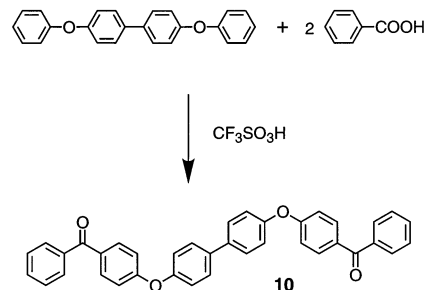


Figure 1. X-ray powder pattern (after subtraction of the amorphous scattering component) for a low molar mass sample of polymer **3** synthesized by the nucleophilic route. The two very weak peaks below $2\theta = 10^\circ$ are thought to arise from the segregation of specific oligomers.

Scheme 3. Synthesis of the Oligomeric Model Compound 10

of essentially the same inherent viscosity, confirming that molar mass in such polycondensations is controlled by solubility rather than stoichiometry. Intense low-angle X-ray scattering (below $2\theta \approx 4^\circ$ for Cu K α radiation) is observed for these polymer samples, reflecting the high degree of microporosity generally associated with polymers crystallized from solution.⁹

Electrophilic syntheses (Scheme 1) using trifluoromethanesulfonic acid as solvent gave polymers of high molar mass (η_{inh} 1.30–1.50 dL g⁻¹) which could be wet-spun into fibers directly from the solutions in which they were formed. The resulting fibers of **3**, **4**, and of their random 1:2 copolymer **5** (all with mp $460 \pm 3\text{ }^\circ\text{C}$)⁵ were oriented at 400 °C by drawing in air to ca. 3.5 times original extension and then annealing at 325 °C at constant length under a nitrogen atmosphere.

As the starting point for structural analyses of **3–5**, an oligomeric model compound (**10**) was synthesized by reaction of 4,4'-diphenoxybiphenyl with excess benzoic acid in trifluoromethanesulfonic acid (Scheme 3), and single crystals were grown by slow cooling of a solution in DMF.

The X-ray structure of **10** revealed a monoclinic unit cell, space group $P2_1/n$, containing four molecules of the oligomer. This adopts a fully extended conformation (Figure 2) with bridge-bond angles averaging 121.5° at the carbonyl groups and 121.8° at the ether linkages. Torsion angles between the aromatic rings and the

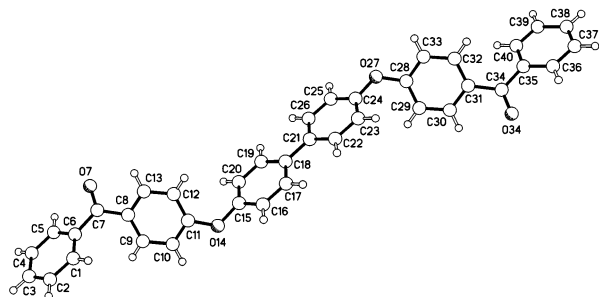


Figure 2. Molecular structure of oligomer **10** from single-crystal data.

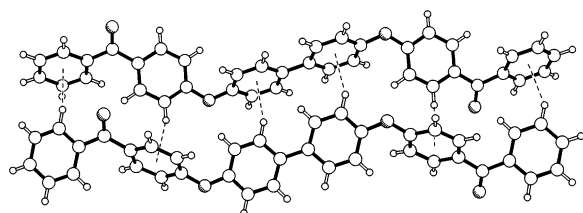


Figure 3. Edge-to-face packing of laterally adjacent chains in the crystal of oligomer **10**.

planes of the bridging units average $28(1)^\circ$ at carbonyl and $32(4)^\circ$ at ether. Despite the absence of a crystallographic inversion center which would *require* the torsion angle between the two rings of the biphenyl unit to be zero, this angle is still less than 1° , with an estimated standard deviation of 0.4° . It is interesting to note that, although planar biphenyl units are energetically unfavorable in the gas phase, crystal packing forces can overcome the barrier to coplanarity,¹⁰ so that both here and in other ether–ketone oligomers containing biphenyl units an essentially coplanar geometry predominates.^{4,11} In the structure of oligomer **10**, the very small asphericity of the anisotropic thermal parameters of the relevant ring atoms (see Supporting Information) clearly demonstrates that coplanarity is not a consequence of the averaging of out-of-plane librations of the two ring systems about their central linking bond, as occurs for example in biphenyl itself.¹²

As shown in Figure 3, laterally adjacent oligomer molecules pack “in register” and are related, in symmetry terms, by an *n*-glide. Planes of aromatic ring systems in adjacent molecules are mutually inclined by $63 \pm 4^\circ$, such that hydrogens of one molecule are directed toward the π -systems of its neighbor with H $\cdots\pi_{\text{centroid}}$ separations ranging from 2.86 to 3.00 Å and C–H $\cdots\pi_{\text{centroid}}$ angles from 132° to 140° . The average intramolecular separation between a carbonyl carbon atom and its nonadjacent ether oxygen is 14.01(1) Å, this distance representing exactly half the molecular repeat distance for polymer **3** and the full repeat distance for polymer **4**.

The information obtained from this single-crystal analysis was used to optimize the Cerius2 “Universal” molecular mechanics force field (Accelrys Inc., San Diego) by redefining optimum bond lengths, bond angles, torsion angles, and Lennard-Jones potentials, such that energy minimization using the modified force field reproduced not only the molecular geometry and conformation of oligomer **10** but also its unit cell to a very good degree of accuracy. A preliminary, fully ordered crystal model for polymer **3** was then constructed in a monoclinic unit cell, retaining the oligomer cell dimensions *a* and *b* and assigning the same rela-

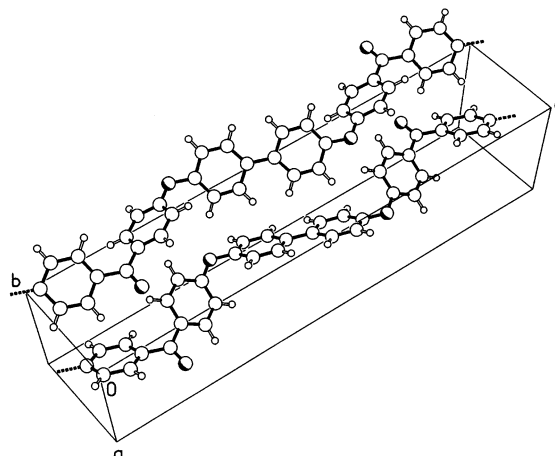


Figure 4. Ordered model for the unit cell of polymer **3**.

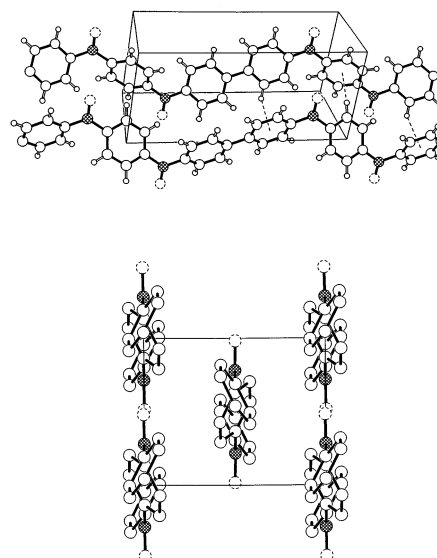


Figure 5. Disordered unit cell available to polymers **3–5**: (a) perspective view; (b) projection along the *c*-direction.

tionship (an *n*-glide) between symmetry-related polymer chains as found for the laterally adjacent oligomer molecules shown in Figure 3. By convention, the *c*-axis was defined parallel to the polymer chain direction. Manual optimization of the polymer unit cell parameters with respect to the experimental X-ray powder pattern and subsequent energy minimization within the optimized cell gave a structure (Figure 4) in the monoclinic (*a*-axis unique) space group *Pb*, with two chains per unit cell [*a* = 7.57(1), *b* = 6.08(1), *c* = 28.09(1) Å, α = $96.6(1)^\circ$].

The X-ray powder pattern simulated from this fully ordered model was generally in very good agreement with the observed data, with the exception of a predicted [001] reflection at *d* = 27.90 Å which could not be identified in the experimental pattern. This predicted reflection does lie in the region where the diffuse low-angle scattering noted above is starting to become significant, but not even a shoulder assignable to [001] could be detected. However, when the crystallographic positions of ether and ketone linkages in the model were *randomized*, as shown in formula **6**, a higher-symmetry crystal (Figure 5) was generated in space group *P2₁/b*, and the 001 reflection was now predicted to be *absent*.

To test the validity of a coplanar biphenyl unit in this structure, the space group symmetry placing an inver-

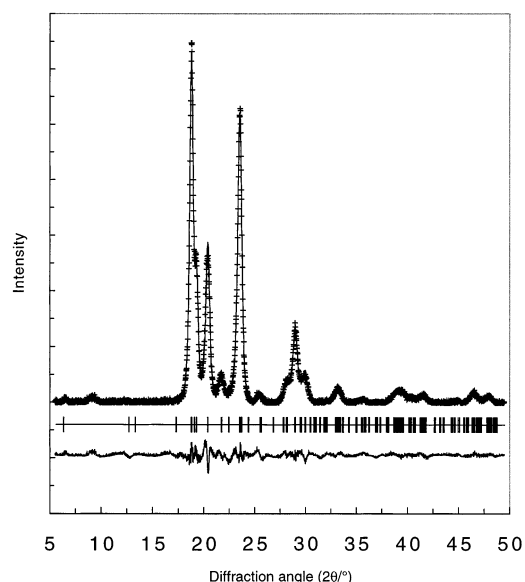


Figure 6. Rietveld difference plot (lower line) for the final, disordered model of polymer **3**. Experimental data (background-subtracted) are shown as + marks, calculated data as a solid line, and calculated peak positions as tick marks.

Table 1. Fractional Atomic Coordinates of the Disordered Model for Polymer 3, in Space Group $P2_1/b$

no.	name	<i>x</i>	<i>y</i>	<i>z</i>
1	C1	0.5835	0.5713	-0.0787
2	C2	0.5812	0.7053	0.0080
3	C3	0.4993	0.6331	0.0870
4	X4 ^a	0.4996	0.7825	0.1788
5	O4 ^b	0.5024	0.9829	0.1765
6	C5	0.5012	0.6936	0.2734
7	C6	0.4217	0.8176	0.3504
8	C7	0.4206	0.7414	0.4396
9	C8	0.5005	0.5413	0.4519
10	C9	0.5814	0.4181	0.3747
11	C10	0.5823	0.4950	0.2856
12	H1A	0.6404	0.6213	-0.1334
13	H2A	0.6385	0.8470	0.0137
14	H6A	0.3655	0.9554	0.3418
15	H7A	0.3653	0.8276	0.4928
16	H9A	0.6376	0.2805	0.3829
17	H10A	0.6378	0.4094	0.2322

^a Superposition of carbon and oxygen atoms (equal weighting).

^b Half-occupancy carbonyl oxygen atom.

sion center at the center of the biphenylene unit was first removed, and the force-field constraint favoring coplanarity was progressively relaxed until free rotation about the biaryl bond was permitted. Even under these conditions, however, reminimization of the model failed to generate any significant torsional rotation about the biaryl bond. Rietveld refinement of the disordered model (unit cell dimensions, crystallite size and strain, and thermal parameters) with respect to the X-ray powder pattern for polymer **3** gave unit cell parameters $a = 7.560$, $b = 6.085$, $c = 14.040$ Å, $\alpha = 96.70^\circ$, and a final agreement factor, R_{wp} , of 5.7%. Simulated and difference powder diffraction patterns for polymer **3** are shown in Figure 6, superimposed on the (background-subtracted) experimental data. Atomic coordinates for the disordered structure, in which bridging units [X=O] represent an averaged superposition of ether and ketone groups, are given in Table 1.

The experimental X-ray powder pattern for polymer **4** was virtually indistinguishable from that of polymer **3**, and indeed Rietveld refinement of the disordered

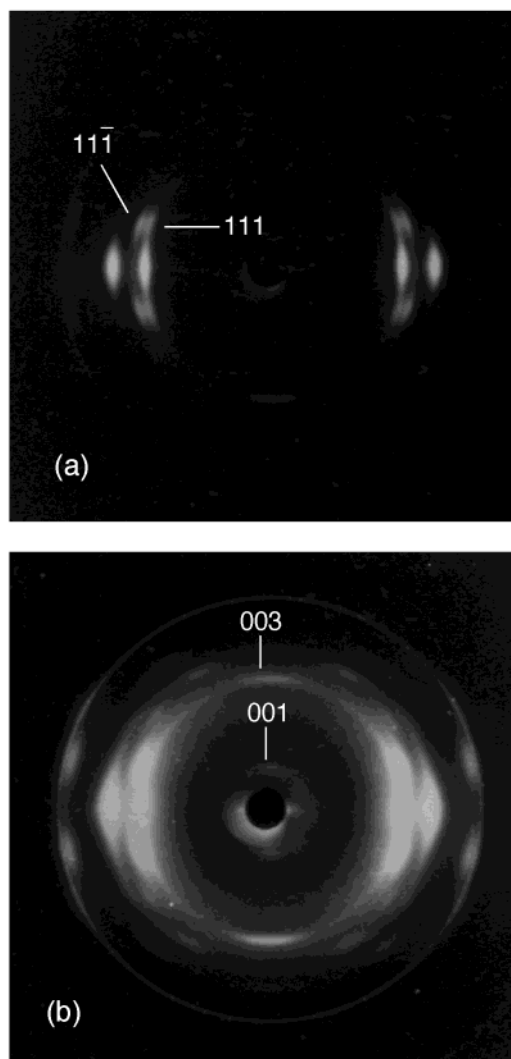


Figure 7. X-ray fiber patterns for polymer **4**: (a) short exposure emphasizing the 111 and $1\bar{1}1$ reflections and (b) long exposure showing a weak, near-meridional 001 reflection characteristic of the ordered phase.

model originally derived for polymer **3**, with respect to the X-ray powder pattern for polymer **4**, gave excellent agreement ($R_{wp} = 6.6\%$) with only very minor changes to the unit cell parameters. Interestingly, although the disordered model predicts that the near-meridional 001 reflection should be absent from the X-ray fiber pattern of **4** (Figure 7a), a long-exposure photograph (Figure 7b) *does* in fact show a weak reflection at this position, suggesting that orientation of polymer **4** induces at least a degree of crystallographic ordering of the ether and ketone linkages. The fiber pattern for the random copolymer **5** showed no reflections associated with ordering of the ether and ketone linkages (as would of course be expected) but was in all other respects identical to those of **3** and **4**.

It is worth commenting at this point that the crystal system and unit cell established for polymers **3** and **4** in this work differ markedly from those recently proposed by Mo et al. (orthorhombic; cell dimensions $a = 7.64$, $b = 6.00$, $c = 13.42$ Å).⁶ The crystallographic convention which places the *c*-axis parallel to the polymer chain direction means that the length of this axis *must* be a direct function of the polymer chain repeat distance. The *c*-axis of the orthorhombic cell assigned by these workers at 13.40 Å is however

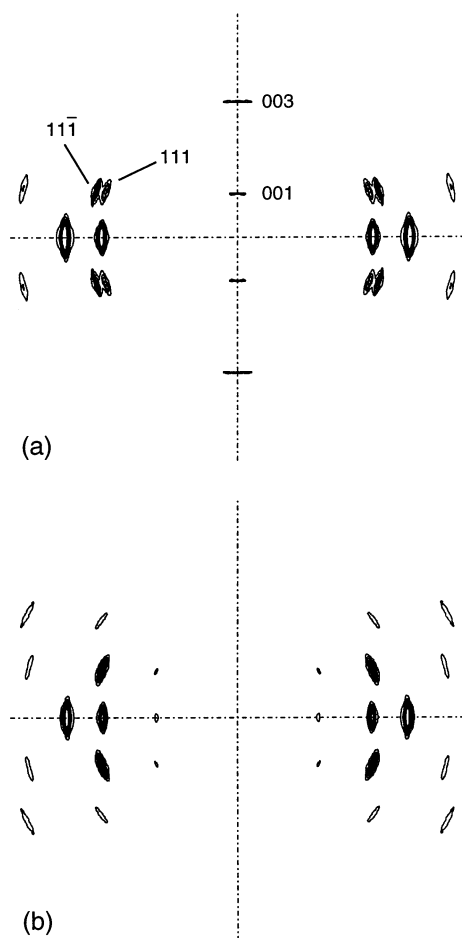


Figure 8. Simulated X-ray fiber patterns for (a) the structure described here for polymer **4** (ordered version) and (b) the structure for polymer **4** proposed in ref 6. These patterns should be compared the experimental data shown in Figure 7.

incompatible with the structural repeat distance determined here from single-crystal oligomer data. Moreover, as described above, we find that a monoclinic unit cell with a *c*-axis length of 14.09 Å must be adopted to accommodate both the polymer diffraction data and a polymer molecule with the preferred geometric and conformational parameters established in our oligomer study. In addition, simulation of fiber patterns from the two different cells clearly demonstrates the requirement for a *monoclinic* unit cell, as this symmetry accurately reproduces the splitting of the 111 and 11 $\bar{1}$ reflections on the first layer line (Figures 7a and 8a), whereas the orthorhombic model suggested by Mo et al. emphatically does not (Figure 8b). These observations highlight the dangers associated with assigning crystal systems and unit cells in the absence of reliable molecular models and reemphasize the importance of diffraction simulation in structural analysis of crystalline polymers.^{2,13}

Finally, it should be noted that the *a*-dimension of the unit cell for *high* molar mass **3**, **4**, and **5** (determined

here from fiber data) is, at 7.76 Å, some 3% larger than corresponding values determined for both oligomer **10** and for the low molar mass samples of these polymers produced by nucleophilic polycondensation. Molar-mass-related variations in *a* have however been reported for a number of aromatic poly(ether ketone)s and their oligomers, and it now seems to be accepted that these can be attributed to the onset of chain folding in the high-molar-mass materials, resulting in an increased lateral stress within the crystallite and thus to an expansion of the lattice.^{14,15}

Conclusions

New types of crystallographically ordered and disordered structures have been identified for biphenyl-based aromatic poly(ether ketone)s using X-ray single-crystal oligomer data interfaced to molecular modeling and diffraction simulation methods. These results clearly demonstrate a requirement for monoclinic rather than the previously proposed orthorhombic symmetry and reemphasize the importance of diffraction simulation in the determination of polymer structure.

Supporting Information Available: Full crystallographic data for the single-crystal X-ray structure of oligomer **10**. This material is available free of charge via the Internet at <http://pubs.acs.org>.

References and Notes

- (1) Hanna, S.; Coulter, P. D.; Windle, A. H. *J. Chem. Soc., Faraday Trans.* **1995**, *91*, 2615.
- (2) (a) Colquhoun, H. M.; Williams, D. J. *Acc. Chem. Res.* **2000**, *33*, 189. (b) Colquhoun, H. M.; Aldred, P. L.; Kohnke, F. H.; Herbertson, P. L.; Baxter, I.; Williams, D. J. *Macromolecules* **2002**, *35*, 1685.
- (3) Dawson, P. C.; Blundell, D. J. *Polymer* **1980**, *21*, 577.
- (4) (a) Colquhoun, H. M.; Dudman, C. C.; Blundell, D. J.; Bunn, A.; Mackenzie, P. D.; McGrail, P. T.; Nield, E.; Rose, J. B.; Williams, D. J. *Macromolecules* **1993**, *26*, 107. (b) Colquhoun, H. M.; O'Mahoney, C. A.; Williams, D. J. *Polymer* **1993**, *34*, 218.
- (5) Colquhoun, H. M.; Lewis, D. F. *Polymer* **1988**, *29*, 1902.
- (6) Qiu, Z.; Mo, Z.; Zhou, H.; Zhang, H.; Wu, Z. *Macromol. Chem. Phys.* **2001**, *202*, 1862.
- (7) Colquhoun, H. M.; Daniels, J. A.; Lewis, D. F. US Patent 4,777,300, 1988, to ICI.
- (8) Shibata, M.; Yosomiya, R.; Zheng, Y.-B.; Ke, Y.-C. *Macromol. Chem. Phys.* **1996**, *197*, 3297.
- (9) Statton, W. O. *J. Polym. Sci.* **1962**, *58*, 205.
- (10) Rabias, I.; Langlois, C.; Provata, A.; Howlin, B. J.; Theodoru, D. N. *Polymer* **2002**, *43*, 185.
- (11) Baxter, I.; Colquhoun, H. M.; Kohnke, F. H.; Lewis, D. F.; Williams, D. J. *Macromolecules* **2002**, *35*, 1685.
- (12) Lenstra, A. T. H.; Vanalsenoy, C.; Verhulst, K.; Geise, H. J. *Acta Crystallogr., Sect. B: Struct. Sci.* **1994**, *B50*, 96.
- (13) (a) Colquhoun, H. M.; Lewis, D. F.; Williams, D. J. *Polymer* **1999**, *40*, 5415. (b) Colquhoun, H. M.; Lewis, D. F.; Williams, D. J. *Macromolecules* **1999**, *32*, 3384.
- (14) Hoffman, J. D.; Miller, R. L.; Marand, H.; Roitman, D. B. *Macromolecules* **1992**, *25*, 2221.
- (15) Baxter, I.; Colquhoun, H. M.; Kohnke, F. H.; Lewis, D. F.; Williams, D. J. *Polymer* **1999**, *40*, 607.

MA020910W